Inorganic Chemistry

pubs.acs.org/IC

Communication

Holmium(III) Single-Ion Magnet for Cryomagnetic Refrigeration Based on an MRI Contrast Agent Derivative

Borja Rodríguez-Barea, Júlia Mayans, Renato Rabelo, Adrián Sanchis-Perucho, Nicolás Moliner, José Martínez-Lillo,* Miguel Julve, Francesc Lloret, Rafael Ruiz-García, and Joan Cano*

Cite This: *Inorg. Chem.* 2021, 60, 12719−12723

Read Online

ACCESS | Metrics & More | Article Recommendations | Supporting Information

ABSTRACT: The coexistence of field-induced blockage of the magnetization and significant magnetocaloric effects in the low-temperature region occurs in a mononuclear holmium(III) diethylenetriamine-*N*,*N*,*N*′,*N*″,*N*″-pentaacetate complex, whose gadolinium(III) analogue is a commercial MRI contrast agent. Both properties make it a suitable candidate for cryogenic magnetic refrigeration, thus enlarging the variety of applications of this simple class of multifunctional molecular nanomagnets.

Mononuclear complexes of lanthanide(III) ions exhibiting slow relaxation of the magnetization, so-called lanthanide single-ion magnets (SIMs), have attracted much attention in diverse areas of nanoscience and nanotechnology.[1−7] Because of their well-known magnetothermal and quantum coherence properties, mononuclear gadolinium(III), dysprosium(III), and holmium(III) derivatives are illustrative examples of the promising applications of Ln SIMs as both molecular cryomagnetic coolants and qubits for cryogenic magnetic refrigeration (CMR) and quantum information processing technologies.[8−11] In the search for molecular materials that exhibit various physical properties linked to technological applications, choosing a starting molecule with one of these properties should be a good strategy.

In this context, we have turned our eyes toward the well-known family of mononuclear complexes with Ln^{III} ions (Ln = Gd, Dy, and Ho) and either linear or cyclic polyaminocarboxylate ligands, widely investigated as magnetic resonance imaging (MRI) contrast agents (Scheme S1).[12,13] Herein we report our first results along this line covering the synthesis, structural, and general physicochemical characterization of the novel holmium(III) diethylenetriamine-*N*,*N*,*N*′,*N*″,*N*″-pentaacetate (DTPA) complex of the formula $Na_2[Ho^{III}(DTPA)(H_2O)]\cdot 8H_2O$ (**1**), as well as a preliminary investigation of the magnetic field dependence of its magnetic and magnetothermal properties through direct-current (dc) and alternating-current (ac) magnetic measurements. Compound **1** constitutes a unique example of Ho^{III} SIM that would operate as a cryomagnetic coolant close enough to the strategically relevant hydrogen liquefaction temperature.

1 was prepared from the stoichiometric reaction of H_5DTPA and holmium(III) oxide in water under reflux for several hours after neutralization with $NaHCO_3$ until pH ca. 6.5 (see the experimental section and Figures S1−S3). X-ray-suitable pale-pink prisms were obtained after several weeks of slow evaporation at room temperature. It crystallizes in the $P2_1/n$ space group of the monoclinic system (Table S1). The asymmetric unit consists of two sodium(I)-bridged dianionic mononuclear $[Ho^{III}(DTPA)(H_2O)]^{2-}$ units, as shown in Figure 1. The two crystallographically independent nine-coordinate Ho1 and Ho2 atoms exhibit similar spherically distorted geometries intermediate between a tricapped trigonal prism (TCTPR) and a monocapped square antiprism

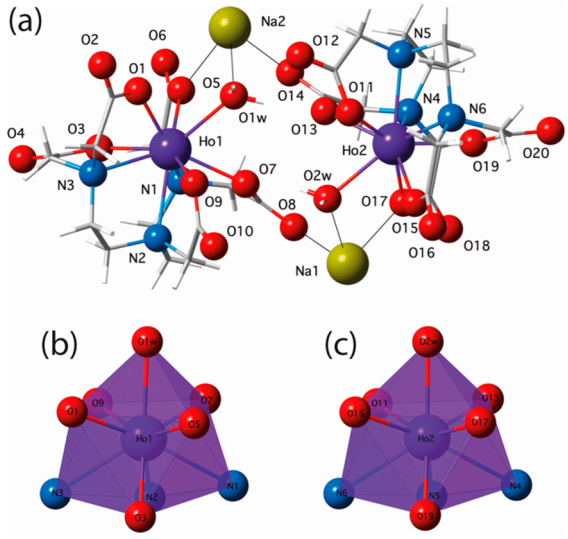

Figure 1. Perspective view of the diholmium(III) entity in **1** (a) showing the double sodium(I)-bridged mononuclear units with the atom numbering scheme. The remaining Na and O atoms from the sodium(I)-coordinated and hydrogen-bonded crystallization water molecules are omitted for clarity. Solid lines represent the Na−O bonds. Views of the metal coordination polyhedra for the two crystallographically independent Ho1 (b) and Ho2 (c) atoms.

Received: June 23, 2021
Published: August 23, 2021

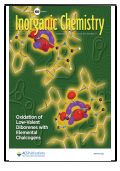

https://doi.org/10.1021/acs.inorgchem.1c01905
Inorg. Chem. 2021, 60, 12719−12723

(CSAPR) of D_{3h} and C_{4v} symmetry (Scheme S2 and Table S2).[14,15] The values of the shape measures for the Ho1/Ho2 atoms are S(TCTPR) = 1.150/1.000 and S(CSAPR) = 1.083/1.089 (S = 0 for a perfect match with the ideal polyhedron), supporting the previous conclusion.[16]

The diholmium(III) entities are further connected through the six-coordinate (Na1 and Na2) and five-coordinate (Na3) Na atoms to give a carboxylate/aqua-bridged sodium(I)−holmium(III) layer of mixed square-decagonal topology growing within the crystallographic *ab* plane (Figure S4a). The remaining six-coordinate Na4 atoms act as additional bridges between adjacent heterobimetallic $Na^{I}Ho^{III}$ layers to give a pillared-layer three-dimensional (3D) network (Figure S4b), featuring small rectangular pores filled by most of the hydrogen-bonded crystallization water molecules (Figure S5). The Ho1···Ho2 separation (r) through the Na1 and Na2 bridges is 6.414 Å, while the shortest intra- and interlayer $Ho1\cdots Ho1^{I}$ and $Ho2\cdots Ho2^{II}$ separations are 8.190 and 10.074 Å (symmetry codes: I, $-x + {}^{1}/_{2}, -y + {}^{1}/_{2}, -z + {}^{1}/_{2}$; II, $-x, -y, -z$).

The static magnetic properties of **1** have been investigated by variable-temperature (2−300 K) molar dc magnetic susceptibility (χ_M) measurements and variable-temperature (2−20 K) and variable-field (0−8 T) molar magnetization (M) measurements (see the experimental section). The $\chi_M T$ versus T and M versus H/T plots (Figure S6) are typical of a highly anisotropic $^5I_8$ ground state (J = 8 with S = 2 and L = 6) resulting from the large first-order spin−orbit coupling in Ho^{III} ions.[17]

At room temperature, $\chi_M T$ for **1** is 14.40 $cm^3\ mol^{-1}$ K. This value is close to that calculated for one Ho^{III} ion (14.07 $cm^3\ mol^{-1}$ K).[15] Upon cooling, $\chi_M T$ continuously decreases to 5.84 $cm^3\ mol^{-1}$ K at 2.0 K (Figure S6a). Ground $^5I_8$ and first excited $^5I_7$ states are well-separated ($\Delta E = -8\lambda$ with $\lambda_0 = -541$ cm^{-1}) so that the former is the only populated below room temperature.[17] The large deviations of the experimental magnetic susceptibility data from the Curie law are then attributed to the action of the ligand-field (LF) potential on the $^5I_8$ ground state (see the Computational details).[18,19] This LF effect causes the splitting of their 17 components into one singlet (m_J = 0) and eight Kramers doublets (m_J from ±1 to ±8), which is ultimately responsible for the high local magnetic anisotropy of the Ho^{III} ion. This conclusion is further supported by the isothermal magnetization curves in the temperature range 2−20 K (Figure S6b). Hence, the M value at T = 2 K for H = 8 T (6.08 Nβ) is well below the calculated value of the magnetization saturation for one Ho^{III} ion (10 Nβ).[17] Moreover, the isothermal magnetization curves do not superpose and largely deviate from the corresponding Brillouin function for a heptadecet state (solid line in Figure S6b).[17]

The dynamic magnetic properties of **1** have been investigated by variable-temperature (2−7 K) and variable-field (0−1 T) in-phase (χ_M') and out-of-phase (χ_M'') molar ac magnetic susceptibility measurements in the frequency range 1−10 kHz (see the experimental section). The χ_M' and χ_M'' versus T and H plots reveal a large temperature and field dependence of the spin dynamics (Figures 2 and S7 and S8).

In the absence of a dc magnetic field (H = 0), there is an incipient χ_M'' signal with no χ_M' maximum at 10 kHz (Figure S7). However, when a relatively small dc magnetic field is applied, χ_M'' shows maxima in the temperature range 2−4 K, with 0.25 T being the optimal working magnetic field (Figure 2). Likewise, a maximum appears in the χ_M'' versus H plots

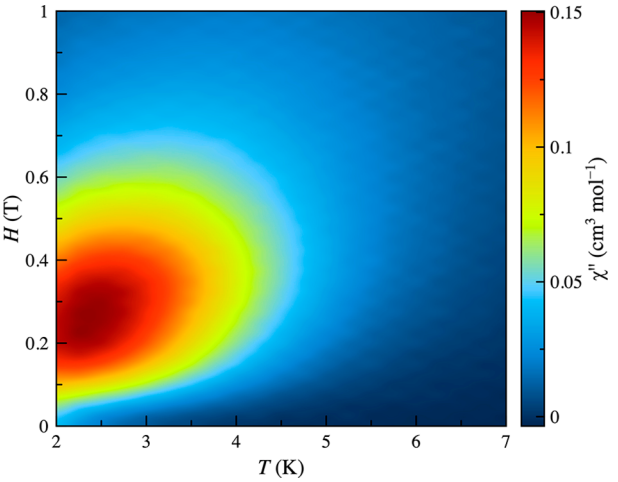

Figure 2. 3D contour color map for the temperature and field dependence of χ_M'' for **1** at 10 kHz of the ±5 Oe oscillating field in the magnetic field and temperature ranges 0−1 T and 2−7 K.

that broadens below 4 K (Figure S8b), showing the appearance of a second competing relaxation process that is clearly noticeable only at 2 K ($H \approx 0.2$ T). These field-induced slow magnetic relaxation (SMR) effects are typical of Ln SIMs, as was earlier reported for the related complexes of the formulas $Na[Gd^{III}(EDTA)(H_2O)_3]\cdot 5H_2O$ and $Na[Dy^{III}(DOTA)(H_2O)]\cdot 4H_2O$ (Scheme S1).[20−22]

To confirm the occurrence of field-induced SIM behavior, the influence of the frequency on the spin dynamics was then investigated at the optimum applied dc magnetic field. The χ_M' and χ_M'' versus T and ν plots in the frequency range 1−10 kHz at H = 0.25 T are compared in Figures S9 and S10. The magnetic relaxation time (τ) values for **1** in the temperature range 2.25−4 K at H = 0.25 T can be calculated from a joint analysis of the χ_M and χ_M'' versus ν plots through the generalized Debye equations, where α describes the distribution of the magnetic relaxation times (solid lines in Figures S9 and S10). The moderate α values in the range 0.36−0.44 support a wide distribution of magnetic relaxation processes (0 and 1 for single and infinite magnetic relaxation processes).

The estimated τ values at H = 0.25 T are represented in the form of the ln τ versus $1/T$ (so-called Arrhenius) plots in Figure S11. The experimental data follow a linear Arrhenius law characteristic of a single thermally activated magnetic relaxation process that was satisfactorily simulated through a two-phonon Orbach mechanism [$\tau^{-1} = \tau_0^{-1} \exp(-U_{eff}/k_B T)$]. The ln τ versus ln T plot does not show any temperature region in which direct relaxation prevails (data not shown). The values of τ_0 and U_{eff} [$3.2(4) \times 10^{-8}$ s and 6.8(2) cm^{-1}] are within the wide range found for the other few examples of Ho SIMs (Table S3).[23−31]

The magnetothermal properties of **1** have been investigated by variable-temperature (2−20 K) and variable-field (0−8 T) magnetization measurements (Figure S12). The resulting magnetic entropy change ($-\Delta S_M$) versus T and ΔH plots obtained through a numerical approach described elsewhere according to the Maxwell equation [$\Delta S_M = \int (\partial M/\partial T)\, dH$] are depicted in Figures 3 and S13.[32]

The contour map in Figure 3 indicates that the optimal working temperature is 9.5 K, reaching a CMR performance higher than 75% for ΔH > 4 T or 50% at 2 K for ΔH = 2 T because of the rapid saturation of the magnetic entropy.

https://doi.org/10.1021/acs.inorgchem.1c01905
Inorg. Chem. 2021, 60, 12719−12723

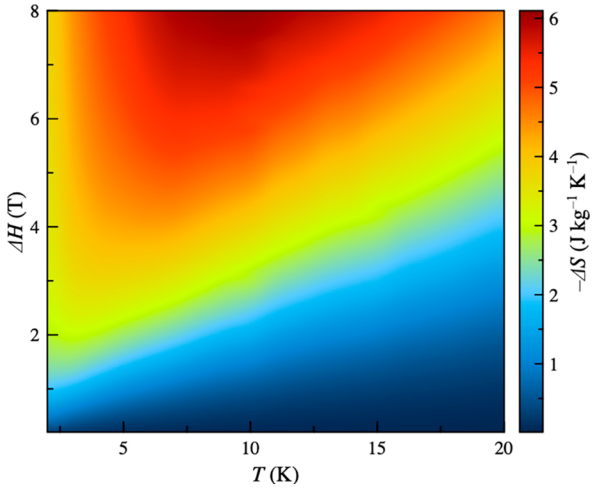

Figure 3. Contour color map for the temperature and field dependence of the $-\Delta S_M$ for **1** in the field and temperature ranges 0−8 T and 2−20 K.

Indeed, high magnetic entropy global changes and large slopes of the isothermal magnetic entropy curves are mandatory for potential applications as molecular cryomagnetic coolants.

Blockage of the magnetization at low temperatures under a weak dc magnetic field (T_B < 2.5 K for H = 0.25 T) should preclude the observation of large magnetocaloric effects (MCEs), as suggested by the lack of a $-\Delta S_M$ maximum for ΔH < 1 T. The increase of the magnetic field induces a progressive shift of this maximum covering a wide temperature range above the liquid-helium temperature, from 3.2 (ΔH = 2 T) to 9.5 K (ΔH = 8 T) (Figure S13a). This feature is also related to the MCE efficiency and eventually to the practical applications of **1** as a cryomagnetic coolant in the low temperature range. By comparison, the mononuclear gadolinium(III) polyoxometalates of the formulas $Na_9[Gd(W_5O_{18})_2]$ and $K_{12}[Gd(P_5W_{30}O_{110})(H_2O)]$, abbreviated as GdW_{10} and GdW_{30}, exhibit SMR effects at very low temperatures (T_B < 0.1 K) in the absence of a magnetic field, with $-\Delta S_M$ maxima just below the liquid-helium temperature.[8,9]

The magnetic entropy increases with the magnetic field, and it tends asymptotically to a thermally dependent value reached more quickly at lower temperatures (Figure S13b). Hence, the maximum $-\Delta S_M$ value in gravimetric units for ΔH = 8 T increases from 4.5 (T = 20 K) up to 6.2 J kg^{-1} K^{-1} (T = 10 K), and then it further decreases to 3.8 J kg^{-1} K^{-1} (T = 2 K). These values are higher than those found for GdW_{10} and GdW_{30} ($-\Delta S_M$ = 1.9 and 4.7 J kg^{-1} K^{-1} at T = 1.3 and 1.8 K, respectively, for ΔH = 7 T),[9] comparing well with those of metallic holmium and related intermetallic alloys (HoB_2 and $HoAl_2$), recently proposed as cryomagnetic coolants just above the hydrogen liquefaction temperature.[33−35]

Yet the maximum $-\Delta S_M$ value in molar units for **1** ($-\Delta S_M$ = 4.7 J mol^{-1} K^{-1} at T = 10 K for ΔH = 8 T) is rather lower than the limiting value for one Ho^{III} ion with no zero-field splitting (zfs) [$\Delta S_M = R \ln(2J + 1)$ = 23.6 J mol^{-1} K^{-1} with J = 8]. Although the Ho^{III} ion possesses the highest total angular momentum along the lanthanide series, this almost 5-fold reduction of the MCE efficiency is expected because of its rather high magnetic anisotropy, as discussed above. In fact, the large zfs of the ground heptadecet state strongly minimizes the magnetic entropy at zero field, thereby reducing the maximal magnetic entropy change (in absolute value) under the application of a magnetic field.

In summary, **1** behaves as a novel Ln SIM with a significant field dependence of the SMR at relatively low blocking temperatures. Likewise, it exhibits moderate MCE in a wide temperature range just above the occurrence of the field-induced magnetization blockage, with strong field-dependent magnetic entropy maxima between the liquid helium and hydrogen temperatures. Despite their limited CMR performance, the results reported herein illustrate the potential of magnetically anisotropic holmium(III)-based SIMs as prototypes of molecular cryomagnetic coolants operating near the strategically relevant hydrogen liquefaction temperature.

■ ASSOCIATED CONTENT

Supporting Information

The Supporting Information is available free of charge at https://pubs.acs.org/doi/10.1021/acs.inorgchem.1c01905.

Synthetic, structural, magnetic, and magnetocaloric data (Tables S1−S3, Schemes S1 and S2, and Figures S1−S13) (PDF)

Accession Codes

CCDC 2069070 contains the supplementary crystallographic data for this paper. These data can be obtained free of charge via www.ccdc.cam.ac.uk/data_request/cif, or by emailing data_request@ccdc.cam.ac.uk, or by contacting The Cambridge Crystallographic Data Centre, 12 Union Road, Cambridge CB2 1EZ, UK; fax: +44 1223 336033.

■ AUTHOR INFORMATION

Corresponding Authors

Joan Cano − *Instituto de Ciencia Molecular/Departament de Química Inorgànica, Facultat de Química, Universitat de València, Paterna, València 46980, Spain;* orcid.org/0000-0002-7382-7135; Email: joan.cano@uv.es

José Martínez-Lillo − *Instituto de Ciencia Molecular/Departament de Química Inorgànica, Facultat de Química, Universitat de València, Paterna, València 46980, Spain;* Email: f.jose.martinez@uv.es

Authors

Borja Rodríguez-Barea − *Instituto de Ciencia Molecular/Departament de Química Inorgànica, Facultat de Química, Universitat de València, Paterna, València 46980, Spain;* Present Address: Weizmann Institute of Science, Rehovot, Israel

Júlia Mayans − *Instituto de Ciencia Molecular/Departament de Química Inorgànica, Facultat de Química, Universitat de València, Paterna, València 46980, Spain;* orcid.org/0000-0001-8875-8075

Renato Rabelo − *Instituto de Ciencia Molecular/Departament de Química Inorgànica, Facultat de Química, Universitat de València, Paterna, València 46980, Spain*

Adrián Sanchis-Perucho − *Instituto de Ciencia Molecular/Departament de Química Inorgànica, Facultat de Química, Universitat de València, Paterna, València 46980, Spain*

Nicolás Moliner − *Instituto de Ciencia Molecular/Departament de Química Inorgànica, Facultat de Química, Universitat de València, Paterna, València 46980, Spain*

Miguel Julve − *Instituto de Ciencia Molecular/Departament de Química Inorgànica, Facultat de Química, Universitat de València, Paterna, València 46980, Spain*

Francesc Lloret − *Instituto de Ciencia Molecular/ Departament de Química Inorgànica, Facultat de Química, Universitat de València, Paterna, València 46980, Spain*
Rafael Ruiz-García − *Instituto de Ciencia Molecular/ Departament de Química Inorgànica, Facultat de Química, Universitat de València, Paterna, València 46980, Spain*

Complete contact information is available at: https://pubs.acs.org/10.1021/acs.inorgchem.1c01905

Author Contributions

The manuscript was written through contributions of all authors. All authors have given approval to the final version of the manuscript.

Funding

This work was supported by the Spanish Ministry of Science, Innovation and Universities (MICIU; Project PID2019-109735GB-I00 and Unidad de Excelencia María de Maeztu CEX2019-000919-M) and the Generalitat Valenciana (AICO/2020/183).

Notes

The authors declare no competing financial interest.

■ ACKNOWLEDGMENTS

A.S.-P. and R.R. thank the MICIU and the Generalitat Valenciana for doctoral grants (FPU/2017/02638 and GRISOLIA/2017/057). J.M. acknowledges the MICIU for a Juan de la Cierva contract.

■ REFERENCES

(1) Luis, F.; Evangelisti, M. Magnetic Refrigeration and Spin-Lattice Relaxation in Gadolinium-Based Molecular Nanomagnets. *Struct. Bonding (Berlin, Ger.)* **2014**, *164*, 431−460.
(2) Dreiser, J. Molecular Lanthanide Single-Ion Magnets: From Bulk to Submonolayers. *J. Phys.: Condens. Matter* **2015**, *27*, 183203.
(3) McAdams, S. G.; Ariciu, A.-M.; Kostopoulos, A. K.; Walsh, J. P. S.; Tuna, F. Molecular Single-Ion Magnets Based on Lanthanides and Actinides: Design Considerations and New Advances in the Context of Quantum Technologies. *Coord. Chem. Rev.* **2017**, *346*, 216−239.
(4) Long, J.; Guari, Y.; Ferreira, R. A. S.; Carlos, L. D.; Larionova, J. Recent Advances in Luminiscent Lanthanide Based Single-Molecule Magnets. *Coord. Chem. Rev.* **2018**, *363*, 57−70.
(5) Zhu, Z.; Guo, M.; Li, X.-L.; Tang, J. Molecular Magnetism of Lanthanide: Advances and Perspectives. *Coord. Chem. Rev.* **2019**, *378*, 350−364.
(6) Jia, J.-H.; Li, Q.-W.; Chen, Y.-C.; Liu, J.-L.; Tong, M.-L. Luminiscent Single-Molecule Magnets Based on Lanthanides: Design Strategies, Recent Advances and Magneto-Luminescent Studies. *Coord. Chem. Rev.* **2019**, *378*, 365−381.
(7) Parker, D.; Suturina, E. A.; Kuprov, I.; Chilton, N. F. How the Ligand Field in Lanthanide Coordination Complexes Determines Magnetic Susceptibility Anisotropy, Paramagnetic NMR shift, and Relaxation Behavior. *Acc. Chem. Res.* **2020**, *53*, 1520−1534.
(8) Martínez-Pérez, M.-J.; Cardona-Serra, S.; Schlegel, C.; Moro, F.; Alonso, P. J.; Prima-García, H.; Clemente-Juan, J. M.; Evangelisti, M.; Gaita-Ariño, A.; Sesé, J.; van Slageren, J.; Coronado, E.; Luis, F. Gd-Based Single-Ion Magnets with Tunable Magnetic Anisotropy: Molecular Design of Spin Qubits. *Phys. Rev. Lett.* **2012**, *108*, 247213.
(9) Martínez-Pérez, M.-J.; Montero, O.; Evangelisti, M.; Luis, F.; Sesé, J.; Cardona-Serra, S.; Coronado, E. Fragmenting Gadolinium: Mononuclear Polyoxometalate-Based Magnetic Coolers for Ultra-Low Temperatures. *Adv. Mater.* **2012**, *24*, 4301−4305.
(10) Pedersen, K. S.; Ariciu, A.-M.; McAdams, S.; Weihe, H.; Bendix, J.; Tuna, F.; Piligkos, S. Toward Molecular 4f Single-Ion Magnet Qubits. *J. Am. Chem. Soc.* **2016**, *138*, 5801−5804.
(11) Shiddiq, M.; Komijani, D.; Duan, Y.; Gaita-Ariño, A.; Coronado, E.; Hill, S. Enhancing Coherence in Molecular Spin Qubits via Atomic Clock Transitions. *Nature* **2016**, *531*, 348−351.
(12) Caravan, P.; Ellison, J. J.; McMurry, T. J.; Lauffer, R. B. Gadolinium(III) Chelates as MRI Contrast Agents: Structure, Dynamics, and Applications. *Chem. Rev.* **1999**, *99*, 2293−2352.
(13) Norek, M.; Peters, J. A. MRI Contrast Agents Based on Dysprosium or Holmium. *Prog. Nucl. Magn. Reson. Spectrosc.* **2011**, *59*, 64−82.
(14) Guggenberger, L. J.; Mutterties, E. L. Reaction Path Analysis. 2. The Nine-Atom Family. *J. Am. Chem. Soc.* **1976**, *98*, 7221−7225.
(15) Ruiz-Martínez, A.; Casanova, D.; Alvarez, S. Polyhedral Structures with an Odd Number of Vertices: Nine-Coordinate Metal Compounds. *Chem. - Eur. J.* **2008**, *14*, 1291−1303.
(16) *SHAPE*, version 2.1; Electronic Structure Group, Universitat de Barcelona, 2013.
(17) Kahn, O. *Molecular Magnetism*; VCH Publishers: New York, 1993; Chapter 2.
(18) Rudowicz, C.; Karbowiak, M. Disentagling Intrigate Web of Interrelated Notions at the Interface between the Physical (Crystal Field) Hamiltonians and the Effective (Spin) Hamiltonians. *Coord. Chem. Rev.* **2015**, *287*, 28−63.
(19) Layfield, R. A., Murugesu, M., Eds.; *Lanthanides and Actinides in Molecular Magnetism*; Wiley-VCH Publishers: New York, 2015.
(20) Holmberg, R. J.; Ho, L. T. A.; Ungur, L.; Korobkov, I.; Chibotaru, L. F.; Murugesu, M. Observation of Unusual Slow-Relaxation of the Magnetisation in a Gd-EDTA Chelate. *Dalton Trans.* **2015**, *44*, 20321−20325.
(21) Car, P.-E.; Perfetti, M.; Mannini, M.; Favre, A.; Caneschi, A.; Sessoli, R. Giant Field Dependence of the Low Temperature Relaxation of the Magnetization in a Dysprosium(III)-DOTA Complex. *Chem. Commun.* **2011**, *47*, 3751−3753.
(22) Cucinotta, G.; Perfetti, M.; Luzon, J.; Etienne, M.; Car, P.-E.; Caneschi, A.; Calvez, G.; Bernot, K.; Sessoli, R. Magnetic Anisotropy in a in a Dysprosium(III)-DOTA Single-Molecule Magnet: Beyond Simple Magneto-Structural Correlations. *Angew. Chem., Int. Ed.* **2012**, *51*, 1606−1610.
(23) Ishikawa, N.; Sugita, M.; Wernsdorfer, W. Nuclear Spin Driven Quantum Tunneling of Magnetization in a New Lanthanide Single-Molecule Magnet: Bis(Phthalocyaninato)Holmium Anion. *J. Am. Chem. Soc.* **2005**, *127*, 3650−3651.
(24) Cardona-Serra, S.; Clemente-Juan, J. M.; Coronado, E.; Gaita-Ariño, A.; Camón, A.; Evangelisti, M.; Luis, F.; Martínez-Pérez, M. J.; Sesé, J. Lanthanoid Single-Ion Magnets based on Polyoxometalates with a 5-fold Symmetry: The series $[LnP_5W_{30}O_{110}]^{12-}$ (Ln^{III} = Tb, Dy, Ho, Er. Tm, and Yb). *J. Am. Chem. Soc.* **2012**, *134*, 14982−14990.
(25) AlDamen, M. A.; Cardona-Serra, S.; Clemente-Juan, J. M.; Coronado, E.; Gaita-Ariño, A.; Martí-Gastaldo, C.; Luis, F.; Montero, O. Mononuclear Lanthanide Single-Molecule Magnets based on the Polyoxometalates $[Ln(W_5O_{18})_2]^{9-}$ and $[Ln(\beta_2\text{-}SiW_{11}O_{39})_2]^{13-}$ (Ln^{3+} = Tb, Dy, Ho, Er. Tm, and Yb). *Inorg. Chem.* **2009**, *48*, 3467−3479.
(26) Dreiser, J.; Westerström, R.; Zhang, Y.; Popov, A. A.; Dunsch, L.; Krämer, K.; Liu, S. X.; Decurtins, S.; Greber, T. The Metallofullerene Field-Induced Single-Ion Magnet $HoSc_2N@C_{80}$. *Chem. - Eur. J.* **2014**, *20*, 13536−13540.
(27) Chen, Y.-C.; Liu, J.-L.; Wernsdorfer, W.; Liu, D.; Chibotaru, L. F.; Chen, X.-M.; Tong, M.-L. Hyperfine-Interaction-Driven Suppression of Quantum Tunneling at Zero Field in a Holmium(II) Single-Ion Magnet. *Angew. Chem., Int. Ed.* **2017**, *56*, 4996−5000.
(28) Ma, Y.; Zhai, Y.-Q.; Ding, Y.-S.; Han, T.; Zheng, Y.-Z. Understanding a Pentagonal-Bipyramidal Holmium(III) Complex with a Record Energy Barrier for Magnetisation Reversal. *Chem. Commun.* **2020**, *56*, 3979−3982.
(29) Chen, S.-M.; Zhang, Y.-Q.; Xiong, J.; Wang, B.-W.; Gao, S. Adducts of Tris(alkyl) Holmium(III) Showing Magnetic Relaxation. *Inorg. Chem.* **2020**, *59*, 5835−5844.
(30) Li, L.-L.; Su, H.-D.; Liu, S.; Wang, W.-Z. Enhancing the Energy Barrier by Replacing the Counterions in Two Holmium(III)-

Pentagonal Bipyramidal Single-Ion Magnets. *Dalton Trans.* **2020**, *49*, 6703−6709.
(31) Wang, J.; Zakrzewski, J. J.; Zychowicz, M.; Vieru, V.; Chibotaru, L. F.; Nakabayashi, K.; Chorazy, S.; Ohkoshi, S. Holmium(III) Molecular Nanomagnets for Optical Thermometry Exploring the Luminescence Re-absorption Effect. *Chem. Sci.* **2021**, *12*, 730−741.
(32) Földeàki, M.; Chahine, R.; Bose, T. K. Magnetic Measurements: A Powerful Tool in Magnetic Refrigeration Design. *J. Appl. Phys.* **1995**, *77*, 3528−3537.
(33) Baran, S.; Duraj, R.; Szytula, A. Magnetocaloric Effect and Transition Order in $HoAl_2$. *Acta Phys. Pol., A* **2015**, *127*, 815−817.
(34) De Castro, B.; Terashima, K.; Yamamoto, T. D.; Hou, Z.; Iwasaki, S.; Matsumoto, R.; Adachi, S.; Saito, Y.; Song, P.; Takeya, H.; Takano, Y. Machine-learning-guided Discovery of the Gigantic Magnetocaloric Effect in HoB_2 Near the Hydrogen Liquefaction Temperature. *NPG Asia Mater.* **2020**, *12*, 1−7.
(35) Terada, N.; Mamiya, H. High-Efficiency Magnetic Refrigeration Using Ho. *Nat. Commun.* **2021**, *12*, 1212.

https://doi.org/10.1021/acs.inorgchem.1c01905
Inorg. Chem. 2021, 60, 12719−12723